invited paper for International Conference on Fracture, to be held Dec. 3-7, 2001, Honolulu, Hawaii, Hilton Hotel

EFFECT OF NANOTEXTURING ON INTERFACIAL ADHESION IN MEMS

M. P. de Boer[1], J. A. Knapp[2] and P. J. Clews[3]

Sandia National Laboratories
[1]Intelligent Micromachining, [2]Radiation Solid-Interactions, [3]Silicon Processing Dept.

www.mdl.sandia.gov/Micromachine

ABSTRACT

We demonstrate that the interfacial adhesion between microelectromechanical systems (MEMS) surfaces is in a regime not previously considered by standard models of rough surfaces such as the Fuller-Tabor [1] or Maugis [2] extensions of the theory of elastic contact of rough surfaces [3]. Our experiments and models show that at small roughness values, adhesion is mainly due to van der Waals forces across extensive non-contacting areas and is proportional to 1/(average surface separation)^2. At large roughness values, asperities that nearly bridge the gap become the dominating contributor to the adhesion. These van der Waals contributions to adhesion have been ignored in the above models. They cannot be ignored in MEMS because the surfaces are in close proximity over a long range as a result of the planar deposition technology.

KEYWORDS microcantilevers, interfacial adhesion, surface roughness, van der Waals forces, self-assembled monolayers

INTRODUCTION

MEMS is a recently developed technology in which free standing polycrystalline silicon (polysilicon) thin film structures are actuated electrostatically to form micron-scale complex mechanisms such as resonating sensors, gears, linear racks, pop up mirrors, and mechanical logic [4]. Because of the large surface-to-volume ratio in this regime, surface forces can dominate over inertial forces, causing mechanisms to adhere rather than perform their intended function.

It is well known that surface roughness reduces adhesion of two contacting bodies. Models describing the effect of roughness on adhesion consider only the adhesion at [1] or near [2] areas of real contact. A reduction in adhesion due to enhanced roughness has also been observed in MEMS. For example, polysilicon roughening techniques have been used to reduce the tendency towards adhesion under wet conditions [5,6]. Free standing cantilevers were actuated under dry conditions and the transition from adhered to free cantilevers was detected to estimate adhesion values [7,8]. It was observed that adhesion decreases with increasing surface roughness, and the authors suggested that $\Gamma \sim A/12\pi d_o^2$, where Γ is the adhesion (J/m^2), A is the Hamaker constant representing van der Waals forces, and d_o is the sum of the root mean square (rms) roughness of the two surfaces as measured by atomic force microscopy (AFM). Theoretical analysis considering the fractal nature of surfaces has also shown that adhesive forces decrease with increasing roughness [9,10].

In this work, we employ a joint experimental and modeling approach to address the effect of roughness on adhesion under dry conditions, allowing us to quantitatively address the following outstanding

questions: (1) To what degree is MEMS adhesion controlled by areas of real contact versus by van der Waals forces across non-contacting portions of the surfaces? (2) What is the minimum achievable value of adhesion for contacting bodies with rough surfaces? (3) What is the optimum value of roughness in MEMS?

SAMPLE PREPARATION

Cantilevers were fabricated according to a three mask level process, schematically represented in Fig. 1. Nanotexturing of the lower layer of polysilicon (poly 0 in Fig. 1(a)) was accomplished by thermal oxidation in dry O_2 at 900 °C for increasing times. Table I indicates the times and the rms roughness as measured by AFM. Fig. 2 shows SEM images of the surface textures achieved by this method after the release etch. Two features are noted. First, the main texturing effect is due to grains that protrude upwards from the surface. This occurs because the polysilicon grains are randomly oriented, and dry oxidation in the linear regime proceeds at different rates on different orientations of silicon [11]. Second, the grain boundaries are decorated at increasing oxidation times, giving rise to grooves. These do not contribute significantly to the desired texturing because they do not take up a large percentage of the surface area, and reach below the surface.

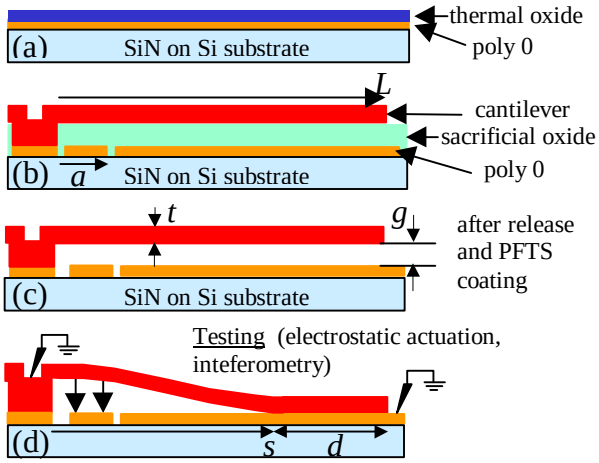

Fig. 1 (a) ground plane polysilicon (poly 0) oxidation (b) cantilever fabrication, (c) release and coating (d) testing

Table I Polysilicon roughness versus oxidation time

Oxdn. Time (min)	Target tox (nm)	rms roughness (nm)
0	--	2.8
20	10	4.5
136	30	7.8
400	60	12.1

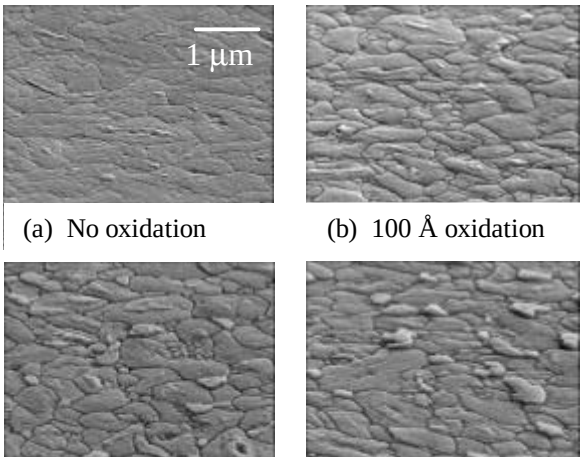

(a) No oxidation (b) 100 Å oxidation

(c) 300 Å oxidation (d) 600 Å oxidation

Fig. 2 Polysilicon ground plane surface textures versus oxidations times (SEM, 70° tilt).

Standard deposition, lithography and etch techniques were used to fabricate the cantilevers (Fig. 1(b)). They are supported on the left in Fig. 1 by a step-up support post, formed by filling a hole etched into the sacrificial oxide layer. A critical step is the release and coating of the cantilevers (Fig. 1(c)). We used a solvent-based coating procedure that applies a self-assembled monolayer coating of perfluorodecyltrichlorosilane (FDTS, ($C_8F_{17}C_2H_4SiCl_3$), similar to ref. [8]. Critical cantilever dimensions, as indicated in Fig. 1, include gap height g, thickness t, width w, length L, and actuation pad length a. After actuation (Fig. 1(d)), the length of the unattached region is used to denote the crack length s. Using profilometry, g=1.90 µm and thickness t=2.62 µm were determined from freestanding cantilevers. Mask dimensions were w=20 µm, a=81.5 µm and L ranged from 100 to 1635 µm.

ADHESION TEST RESULTS

Most cantilevers were free standing at lengths up to 1635 μm after the release and drying procedure as determined by interferometry. Some of these long cantilevers were contacting the substrate at their tips. In a few cases, cantilevers were attached over a relatively long length *d*, as indicated in Fig. 1(d). This latter group was excluded from further analysis.

Knowledge of Young's Modulus *E* and torsional support post compliance *b* are critical to assessing Γ [12]. We used a procedure previously described in detail [13] to determine *E*=163 GPa and *b*=1.25 μrad/(μN•μm). Also small curvatures *k* (caused by stress gradient through the thickness of the film) ranging from 0-1 m^{-1} were measured, and play a secondary role in determining adhesion values. These quantities are determined by electrostatically actuating the cantilevers, measuring the deflections and finding the best fit to finite difference models over a range of applied voltages.

Using a fracture mechanics analogy, a cantilever's adhesion to a substrate can be measured to high sensitivity and accuracy along its length [12,14]. In the adhesion testing procedure, free standing cantilevers are brought into contact with the substrate by modulating the voltage on the actuation pad. Using interferometry, the full deflection curve of the cantilevers is determined to better than 10 nm accuracy. At low to moderate voltages (up to 60V for this geometry), the deflections are highly sensitive to interfacial forces acting between the cantilever and the substrate.

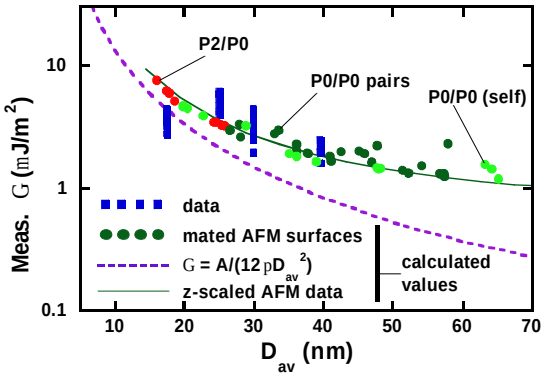

Fig. 3 Experimental and calculated results for adhesion verus average roughness

For different voltages applied to the actuation pad, corresponding to different points along the length of the beam, interferograms were taken and deflection curves were extracted. Knowing *a* and *w* from the mask layout and using the measured data for *E*, *t*, *g*, and *b* as input parameters, adhesion was determined by matching the model to each measured deflection curve. The only free parameter in the modeled curves is the adhesion Γ. A least squares fit between the model and measurement was used to determine its value. Typical minimum errors are less than 5 nm/pixel. Adhesion results for the different surface roughnesses are shown in Fig. 3, where the squares (data) correspond to the measured values of adhesion. The adhesion data is plotted versus D_{av}, the average separation between the surfaces. For each value of D_{av}, Γ values were determined from two different cantilevers at applied voltages of 0, 10, 20, 30, 40, 50 and 60 V. Small systematic errors in the input parameters limit the absolute accuracy of the Γ values to ~10%, but will not affect the relative values of adhesion in Fig. 3.

ANALYSIS

Adhesion testing was conducted in air at ~30% relative humidity (RH). A contact angle of 110° of the FDTS coating with water was measured, indicating a hydrophobic coating. We have observed no effect of RH on testing results up to 80% RH for these coatings [14]. Therefore, capillary condensation, which dominates adhesion of hydrophilic surfaces [15], does not play a role in these experiments. Furthermore, because the top and bottom surfaces are both grounded, electrostatic forces in the contact

zone *d* are insignificant. However, externally applied loads, van der Waals forces between the surfaces and contact at asperities must be considered to analyze our results.

To model the interfacial forces, we measured the topography of the top and bottom surfaces by AFM (double-sided tape applied to the cantilevers allows them to be removed from the substrate and placed upside down for imaging). A question arises as to the area of the contacting region that should be modeled. By considering the free body diagram of the loaded cantilever, there must be a short region of compressive contact just beyond the crack tip. From simple beam mechanics, a point reaction force exists, but from elastic considerations, this region has length ~2*t*, and therefore the contact area should be considered is ~2*tw*=80 μm^2. In fact, 10x10 μm^2 AFM images with 256 or 512 pixels in each direction (e.g., 40 or 20 nm lateral resolution) were used in our analysis.

The AFM topograph data was read into a finite element program, and the top and bottom surfaces were placed in contact in various ways as will be described below. An elastic-plastic model was created to describe the silicon material with *E*=165 GPa and hardness *H*=12 GPa. However, it was soon found that for any reasonable pressure as applied by the external modulation, only the first contacting asperity in the contact zone deforms, and then by less than 0.5 nm. At each pixel, a parallel plate law for van der Waals forces was used to model the adhesive forces, similar to the equation posed in the Introduction, e.g., $\Gamma = A/(12\,p\,D_o^2)$. However, D_o now replaces d_o, where D_o represents the gap at each individual pixel, and the adhesion energy is summed up over the individual pixels and divided by the total area. For the few pixels where there is actual contact, a cutoff value of D_{oc} =0.3 nm [16] was used. With $A=5 \bullet 10^{-20}$ J for a fluorocarbon surface, a surface energy of 15 mJ/m^2 is calculated in these regions. For comparison, values of 7 and 28 mJ/m^2 for advancing and receding surface energies respectively were recently determined by surface force apparatus measurements for a fluorocarbon surfactant (TAFC, $(C_8F_{17}C_2H_4)_2$-L-Glu-Ac-N^+-$(CH_3)_3$-Cl^-) applied to a mica surface.

The surfaces were placed in contact in various combinations. This included the original top and bottom measured layers with various random shifts in alignment, and pairs of the bottom layers including mating of the bottom layer to itself. The circles in Fig. 3 are the calculated adhesion results for the various combinations of the data. The solid line represents data from an individual placement combination, but with the roughness scaled to both lower and higher scales. The value of $D_{av} \approx 2d_o$ in Fig. 3 is determined by the finite element analysis for a given placement of the top and bottom surfaces.

DISCUSSION

The abscissa D_{av} in Fig. 3 is better used than d_o because it takes into account the actual alignment of the two surfaces, thereby reflecting the separation of the associated highest asperity pair. At small D_{av} values, $\Gamma = A/(12\,p\,D_{av}^2)$ is a good approximation for the calculated adhesion (circles in Fig. 3). Of course, this equation will always be a lower bound for the adhesion values because of the non-linearity in this equation. However, as indicated by both the data and the model, the adhesion does not fall off with $1/D_{av}^2$ at large D_{av} values. It is important to realize that for these deposited layers, there is no long range waviness to the surfaces. Therefore, surfaces can be near each other over large distances without contacting.

To qualitatively understand the results, we consider two conceptual extremes in the adhesion between rough surfaces. In one, the surfaces are relatively smooth and contact is at only one asperity point. Van der Waals forces across non-contacting portions of the surfaces, whose area is far greater than the

contacting area at the one asperity, will dominate the adhesion in this case. For example, at D_{av} =10 nm, Γ=13 μJ/m^2 is expected as seen in Fig. 3. At the other extreme, the surfaces are rough, and D_{av} is large. Only the single point of contact contributes to the adhesion. In this case, we would expect $\Gamma \sim (AR/(6D_{oc})/L_c^2)$, where *R* is the radius of the contacting asperities and L_c^2 is the area of adhesion that is being probed (the term $AR/(6D_{oc})$ is the van der Waals adhesion energy between two contacting spheres). With *R*=50 nm as a typical value for the polysilicon asperities in these experiments and L_c^2=100 μm^2 as discussed above, we expect a lower bound for adhesion to be 0.014 μJ/m^2. This latter extreme is a simplified expression of the Maugis model of rough surfaces [2], which takes van der Waals forces into account, but only at contacting asperities. That model is more appropriate here than the Fuller-Tabor approach because of the large *E* and small *R* of these surfaces. Note that the values of adhesion in Fig. 3 are much closer to the former than the latter extreme, implying that van der Waals forces over non-contacting areas dominate the adhesion. Negligible adhesion hysteresis measured in other experiments corroborates this notion [14].

To quantitatively understand the results, consider Fig. 4, where a histogram of the relative contributions from the range of D_o values is plotted for different surface roughnesses. At small D_{av}, most of the contribution to adhesion comes from non-contacting surfaces, whereas at large D_{av}, the contribution from surfaces nearly in contact begins to become the largest contributor.

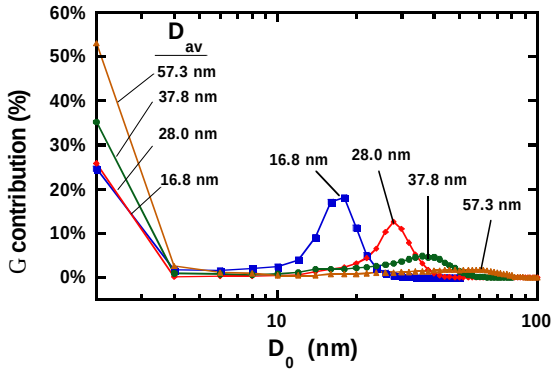

We can now address the questions posed in the Introduction. (1) Typically, MEMS surfaces exhibit D_{av} ~10-30 nm. Therefore, most adhesion in MEMS is due to van der Waals forces between non-contacting areas. Even for large D_{av} in Fig. 3, this remains true - the reason for the small reduction in Γ is that nearby non-contacting asperities begin to contribute significantly to adhesion. However, as D_{av} grows above 60 nm, the Maugis model will adequately describe the adhesion. (2) Adhesion as low as 0.01 μJ/m^2 should be possible by making surfaces rough. However, because of the weak dependence of Γ on D_{av}, extremely large roughness would be required. Given that MEMS structures are often used for optical reflection in mirror applications, this would be an unpopular choice. (3) There is a deviation in the calculated curve from $\Gamma = A/(12\,p\,D_{av}^2)$ beginning at D_{av} ~25 nm. We suggest this is a near-optimal separation value. For lower values of roughness, adhesion begins to increase significantly because of the close proximity of the surfaces, while for large values, optical reflectivity is significantly compromised.

Using the Greenwood-Williamson model [3], which applies reasonably well for these surfaces, the ratio of real to apparent contact area is found to be approximately 10^{-8} for the smoothest surfaces. The real contact area is greatly overestimated in the finite element formulation because of the pixel size limitation. Depending on the lateral resolution used in the AFM measurements, the smallest possible ratio is $(1/256)^2=1.5\bullet 10^{-5}$ or $(1/512)^2=3.8\bullet 10^{-6}$. Because the contribution to the total adhesion of the contacting point is still small, this causes only a small error in the adhesion calculation. However, this is further evidence that van der Waals forces in the vast area between contacts dominates the adhesion of these surfaces, especially when the average separation is small.

SUMMARY AND CONCLUSIONS

Understanding the effects of surface roughness on parameters such as adhesion, friction and wear is a central question in the tribology of MEMS. By combining deflection data from interferometry with computer-based models, the use of as-fabricated MEMS test structures provides a powerful means to the assess the interfacial adhesion between rough surfaces. In this work, we fabricated polysilicon cantilevers over textured surfaces of varying nm scale roughness, and measured the interfacial adhesion of the cantilevers to the surfaces. Contrary to expectations, the effect of roughness, when increased over a large range from 3 to 12 nm rms, reduced the adhesion only by a factor of 2, instead of by a factor of 16 as expected from previous literature models. The adhesion was studied by inputting 3-D data from AFM topographs of the surfaces into a finite element code, and mating the surfaces in the computer. It was found that at small roughness values, adhesion is mainly due to van der Waals forces across non-contacting areas and is proportional to 1/(average surface separation)^2. At large roughnesses, asperities that nearly bridge the gap are the dominating contributor to the adhesion.

ACKNOWLEDGMENTS

Sandia is a multiprogram laboratory operated by Sandia Corporation, a Lockheed Martin Company, for the United States Department of Energy under contract DE-AC04-94AL85000. We thank Aaron Hall for help in obtaining AFM data.

REFERENCES

[1] K. N. G. Fuller and D. Tabor, Proc. Roy. Soc. Lond. A. **345** 327 (1975).
[2] D. Maugis, J. Adh. Sc. Tech. **10** (2) 161 (1996).
[3] J. A. Greenwood and J. B. P. Williamson, Proc. Roy. Soc. Lond. A. **295** 300 (1966).
[4] J. J. Sniegowski and M. P. de Boer, Annu. Rev. Mater. Sci. **30** 297 (2000).
[5] R. L. Alley, P. Mai, K. Komvopoulos and R. T. Howe, Proc. 7th Int. Conf. Solid-State Sensors and Actuators, Transducers '93, Yokohama, Japan, 1993, pp. 288-291.
[6] Y. Yee, K. Chun and J. D. Lee, The 8th Int. Conf. on Solid-State Sensors and Actuators, Transducers '95, Stockholm, Sweden, 1995, pp. 206-209.
[7] M. R. Houston, R. T. Howe and R. Maboudian, J. Appl. Phys. **81** (8) 3474 (1997).
[8] U. Srinivasan, M. R. Houston, R. T. Howe and R. Maboudian, J. Micromech. Sys. **7** (2) 252 (1998).
[9] K. Komvopoulos and W. Yan, J. Trib. **119** 391 (1997).
[10] K. Komvopoulos and W. Wan, J. Appl. Phys. **84** (7) 3617 (1998).
[11] *VLSI Technology*; *Vol.* , edited by S. M. Sze (McGraw-Hill, New York, 1983).
[12] J. A. Knapp and M. P. de Boer, J. MEMS **to be submitted** (2001).
[13] B. D. Jensen, M. P. de Boer, N. D. Masters, F. Bitsie and D. A. LaVan, J. MEMS **10** (3) in press (2001).
[14] M. P. de Boer, J. A. Knapp, T. A. Michalske, U. Srinivasan and R. Maboudian, Acta Mater. **48** (18-19) 4531 (2000).
[15] M. P. de Boer, P. J. Clews, B. K. Smith and T. A. Michalske, Mater. Res. Soc. Proc., San Francisco, CA, 1998, pp. 131-136.
[16] J. Israelachvili, *Intermolecular and Surface Forces* (Academic Press, New York, 1992).